

## Computational Fluid Dynamic Analysis of Plasma Spray Physical Vapor Deposition

Panpan Wang<sup>§</sup>, Wenting He, Georg Mauer, Robert Mücke and Robert Vaßen  
Forschungszentrum Jülich GmbH, Institute of Energy and Climate Research, Jülich, Germany

<sup>§</sup>Correspondence author. Email: p.wang@fz-juelich.de

**ABSTRACT** The plasma spray process has been developed to deposit thin coatings. The plasma jet properties have been investigated by conducting simulations with the ANSYS Fluent 17.1 applying the SST  $k - \omega$  turbulence model. As the inputs of simulations, the required plasma thermodynamic and transport properties are calculated in local chemical equilibrium (LCE) and local thermodynamic equilibrium (LTE). The simulated results of turbulence and temperature of the plasma jet are described. Regarding the experimental results, the analysis of plasma jet's turbulence and Mach disk are also given. However, in the case of consideration of coatings formation, Monte Carlo simulations are used to simulate the growth of columns. And the orientations of columns of the thin films are compared with that of the simulated results.

**Introduction** The plasma spray physical vapor deposition process (PS-PVD) combines very low chamber pressure (200 Pa) and high power input (maximum 180 kW) to obtain a supersonic and high-temperature plasma jet, which could be used to melt and evaporate feedstocks (YSZ) to deposit splat-like or columnar microstructure formation coatings. It is investigated to manufacture solid oxide fuel cells [1, 2], gas separation membranes [3] and thermal barrier coatings [4].

Figure 1 shows the schematic of the simulated plasma jet and its image of 35Ar-60He at chamber pressure 200 Pa. The conditions of all plasma jets images, as shown in Figure 1(c) are took in the corresponding plasma spray process, and the O3CP gun, as shown in Figure 1(b) is employed on a Sulzer Metco LPPS-TF Multicoat System.

**Method** Modelling of the supersonic compressible plasma flow has been developed to describe the thermodynamic and transport properties of the PS-PVD process. The thermodynamic and transport properties of the plasma gas mixtures (35Ar-60He\*) were obtained as a function of temperature and pressure from the thermodynamic calculations in chemical equilibrium (CEA program) with consideration of ionization. Commercial computational fluid dynamics software (ANSYS fluent 17.1) has been used for the simulations. Through a two-dimensional numerical analysis, Pressure-based and SST  $k - \omega$  model is applied to simulate the temperature and turbulence distribution of the plasma plume. Based on user-defined functions, plasma mixture compositions for three different chamber pressures were obtained as inputs to model the plasma jet. Two-dimensional Monte Carlo simulations have been conducted to provide insight into the evolution of columns around the sample. This model is implemented on a molecular scale that incorporates the effect of self-shadowing and vapor incidence angle. Assumptions of simulations are shown as follows: the plasma jet and the chamber have the same

compositions; all zirconia are evaporated and effect of properties of evaporated particles on plasma plume was neglected; the mass flow rate, the composition of plasma forming gas and net power (60 kW) were obtained from the experiment.

\*the unit is standard liter per minute (slpm).

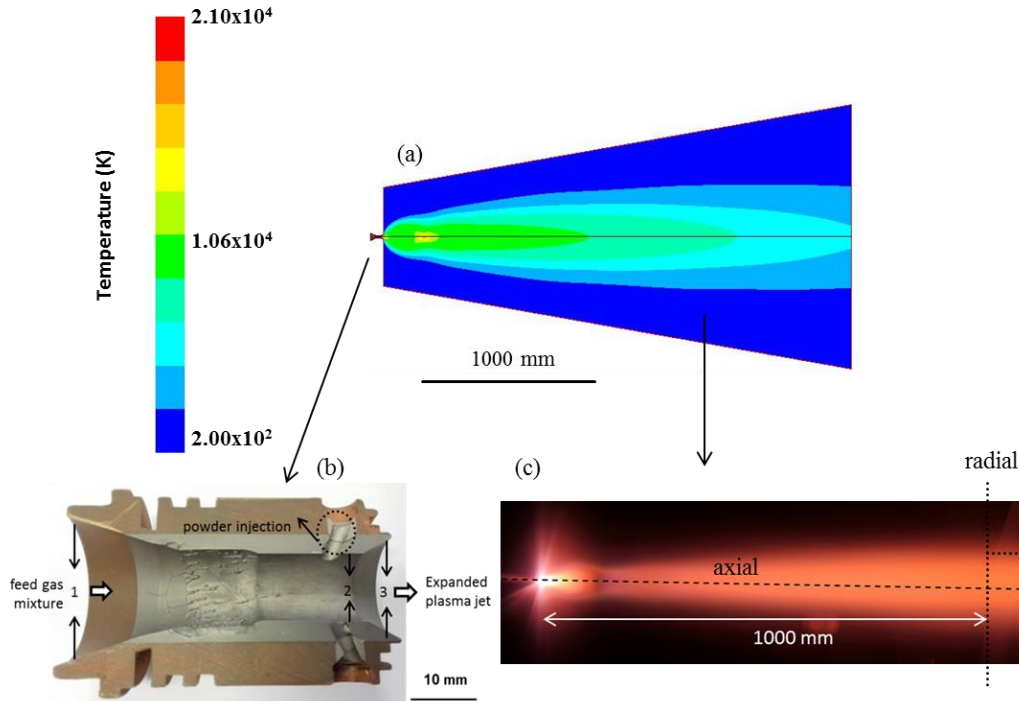


Figure 1. The schematic of the plasma jet of 35Ar-60He at chamber pressure 200 Pa; (a) the simulated temperature contour, (b) the O3CP nozzle, (c) the plasma jet image.

**Results and Discussions** Figure 2 shows the effect of the chamber pressures on plasma jet turbulence, Mach disk and length. The temperature distributions along the axial direction are shown in Figure 2 for different chamber pressures.

Compared between Figure 2 and Figure 3, the jet shock length is 100 mm and 50 mm for chamber pressure 200 Pa and 1,000 Pa, respectively. For the chamber pressure less than 1000 Pa, the temperature can keep quite high and homogeneous for long distance. The jet shock length can be comparable with the images. Temperature decreases along the downstream of plasma jet. In particular, when the chamber pressure is smaller than 4,000 Pa, the phenomena known as Mach disks are high pressure regions in the exhaust from the exit of a jet nozzle. These regions are formed through a repeating and decaying, series of shocks and expansions caused by the difference between the exit pressure around the jet and the chamber pressure. While the chamber pressure is larger than 4,000 Pa, shock diamonds can be clearly observed inside the jet.

Figure 4 depicts the predicted turbulent viscosity ratio and turbulent Reynolds number developments of plasma jet along radial direction at the axial stand-off distance of 500 mm for different chamber pressure. For chamber pressure lower than 1,000 Pa, the jet tends to be laminar. Turbulent viscosity ratio and turbulent Reynolds number increases follows chamber pressure increase. The degree of turbulence not only describes the quantity of cold gas entrained into the jet and thus the volume of useful plasma, but it also affects heat transfer rates to particles travelling through the jet. The maximum turbulent Reynolds number at chamber pressure 1,000 Pa is less than 1,000; while at 6,000 Pa the largest value is 6,000. As depicted in the Figure 2(right), the present study of predicted turbulent values show laminar for chamber pressure less than 1000 Pa.

The comparisons of microstructures and two-dimensional Monte Carlo simulated results are shown in Figure 5. The incoming particles at a certain angle deposit in the sample surface with consideration of self-shadowing effects in the simulation that can be used to simulate the columnar growth.

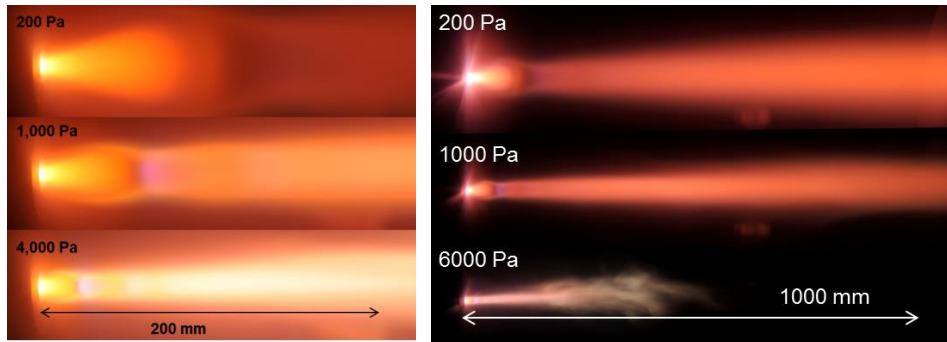


Figure 2. Comparisons of plasma (35Ar-60He) jet images for three different chamber pressures (6,000 Pa, 4,000 Pa, 1,000 Pa and 200 Pa).

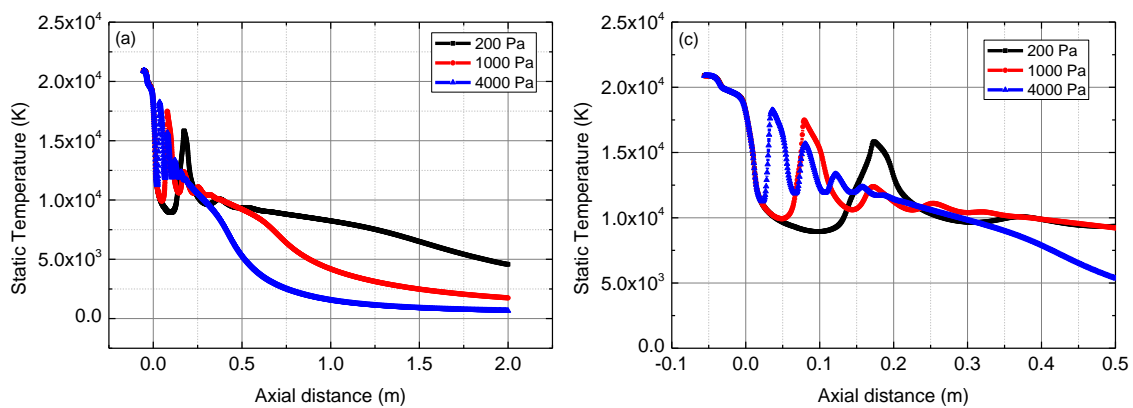


Figure 3. Axial distance dependence of temperature on varied chamber pressure (200 Pa, 1,000 Pa, and 4,000 Pa) of the plasma jet of 35Ar-60He.

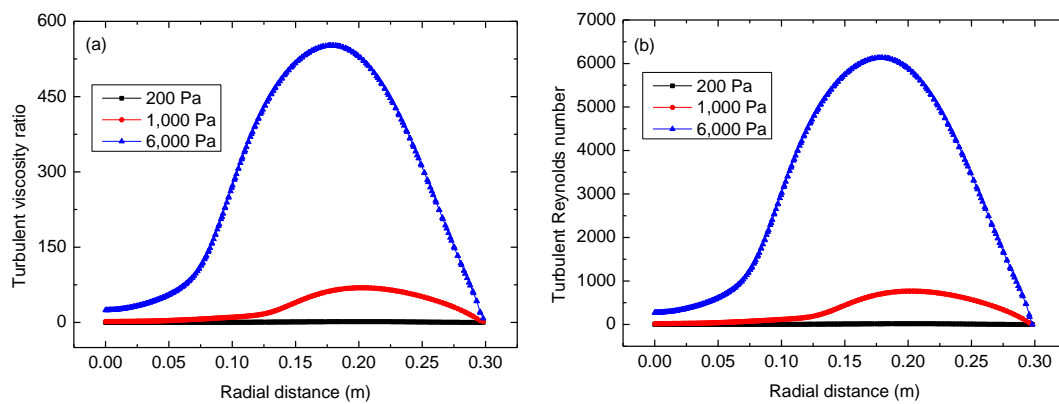


Figure 4. Radial direction dependence of turbulent viscosity ratio and turbulent Reynolds number of the plasma jet on varied chamber pressure (200 Pa, 1,000 Pa, and 6,000 Pa) at the axial stand-off distance of 500 mm of the plasma jet of 35Ar-60He.

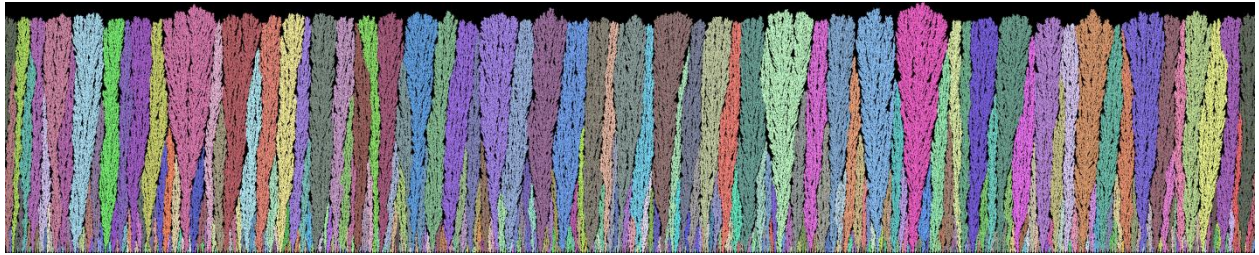
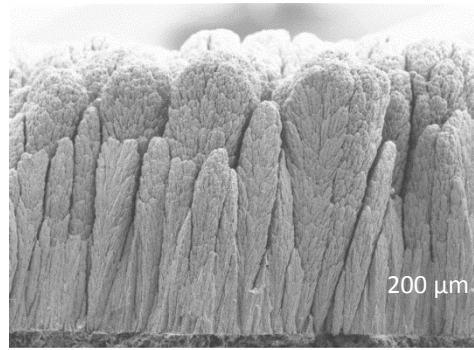


Figure 5. Comparison of microstructure of PS-PVD [5] and simulated results .

Assumptions are made about the formation of columns growth without consideration of long-distance diffusion, as well as limited mobility of big-size incoming particles (clusters).

## References

1. Stöver, D., et al., *Plasma-sprayed components for SOFC applications*. Surface and Coatings Technology, 2006. **201**(5): p. 2002-2005.
2. Hui, R., et al., *Thermal plasma spraying for SOFCs: Applications, potential advantages, and challenges*. Journal of Power Sources, 2007. **170**(2): p. 308-323.
3. Jarligo, M.O., et al., *Plasma Spray Physical Vapor Deposition of  $La_{1-x}Sr_xCo_yFe_{1-y}O_{3-\delta}$  Thin-Film Oxygen Transport Membrane on Porous Metallic Supports*. Journal of Thermal Spray Technology, 2014. **23**(1): p. 213-219.
4. Vassen, R., A. Stuke, and D. Stöver, *Recent Developments in the Field of Thermal Barrier Coatings*. Journal of Thermal Spray Technology, 2009. **18**(2): p. 181-186.
5. Hospach, A., et al., *Characteristics of Ceramic Coatings Made by Thin Film Low Pressure Plasma Spraying (LPPS-TF)*. Journal of Thermal Spray Technology, 2012. **21**(3-4): p. 435-440.